Inorg. Chem. **2005**, *44*, 9097–9104

Multinuclear and Dynamic NMR Study of *trans*-[Pt(Cl)(PHCy$_2$)$_2$(PCy$_2$)], [Pt(Cl)(PHCy$_2$)$_3$][BF$_4$], [Pt(Cl)(PHCy$_2$)$_3$][Cl], *trans*-[Pt(Cl)(PHCy$_2$)$_2${P(S)Cy$_2$}], and *trans*-[Pt(Cl)(PHCy$_2$)$_2${P(O)Cy$_2$}]. Influence of Intramolecular P═O···H–P and Cl···H–P Interactions on Restricted Rotation about Pt–P Bond. X-ray Structure of *trans*-[Pt(Cl)(PHCy$_2$)$_2${P(O)Cy$_2$}]

Piero Mastrorilli,*[†] Cosimo F. Nobile,[†] Mario Latronico,[†,#] Vito Gallo,[†] Ulli Englert,[‡] Francesco P. Fanizzi,[§] and Oronzo Sciacovelli[||]

Dipartimento di Ingegneria delle Acque e di Chimica del Politecnico di Bari, via Orabona 4, I-70125 Bari, Italy, Institut für Anorganische Chemie der RWTH, Landoltweg 1, D-52074 Aachen, Germany, Dipartimento di Scienze e Tecnologie Biologiche e Ambientali, Università di Lecce, Via Monteroni, I-73100, Lecce, Italy, Consortium C.A.R.S.O., Cancer Research Center I-70010, Valenzano-Bari, Italy, and Dipartimento di Chimica dell'Università degli Studi di Bari, via Orabona 4, I-70125 Bari, Italy

Received July 18, 2005

Dynamic NMR experiments on *trans*-[Pt(Cl)(PHCy$_2$)$_2${P(X)Cy$_2$}]^z where X is a lone pair (**1**, $z = 0$), H (**2**, $z = +1$), S (**3**, $z = 0$), or O (**4**, $z = 0$) show that the rotation around the P(X)–Pt bond is hindered for all molecules studied, with $\Delta G^{\ddagger}$ ranging from 8.2 to 11.0 kcal/mol. The highest value of the series was calculated for *trans*-[Pt(Cl)-(PHCy$_2$)$_2${P(O)Cy$_2$}] (**4**) where intramolecular P═O···H–P interactions act as a molecular brake at room temperature. Single-crystal X-ray diffraction confirms the presence of both *intra* and *inter*molecular P═O···H interactions in solid **4**. In the case of [Pt(Cl)(PHCy$_2$)$_3$]Cl, multinuclear NMR analysis indicates the presence of a P–H···Cl$^-$ interaction in aromatic or halogenated solvents which could have also a minor effect on the rotational barrier around the P(X)–Pt bond.

Introduction

Since the extensive work of Bushweller on stereodynamics of the ligand−metal bond,[1] the interest in the dynamic behaviors of transition metal complexes has been uninterrupted, with particular attention being devoted to the study of rotational isomerism caused by restricted rotation around a ligand−metal bond.[2,3] Although the factor on which a restricted rotation around a ligand−metal bond depends is often the bulk of the ligand, nevertheless other causes have been found to participate to the aforementioned dynamic processes, such as arene stacking[3] or the presence of four fairly small phosphanyl ligands in a coordination plane.[4] The preferred technique used in the study of molecular dynamics is NMR, which requires the presence of an NMR active nucleus acting as probe for the slow exchange resulting from the molecular motion in the complex. Typical nuclei used as probes are ^{1}H and ^{31}P but also ^{19}F and ^{13}C have been exploited, for example, in the dynamic study of Pt(dppe)-

* To whom correspondence should be addressed. E-mail: p.mastrorilli@poliba.it.

[†] Dipartimento di Ingegneria delle Acque e di Chimica del Politecnico di Bari.

[‡] Institut für Anorganische Chemie der RWTH.

[§] Università di Lecce and Consortium C.A.R.S.O.

[||] Dipartimento di Chimica dell'Università degli Studi di Bari.

[#] On a leave of absence from Dipartimento di Ingegneria e Fisica dell'Ambiente, Università della Basilicata, viale dell'Ateneo Lucano 10, I-85100 Potenza, Italy.

(1) Bushweller, C. H.; Hoogasian, S.; English, A. D.; Miller, J. S.; Lourandos, M. Z. *Inorg. Chem.* **1981**, *20*, 3448−3455. (b) Bushweller, C. H.; Rithner, C. D.; Butcher, D. J. *Inorg. Chem.* **1984**, *23*, 1967−1970. (c) Bushweller, C. H.; Rithner, C. D.; Butcher, D. J. *Inorg. Chem.* **1986**, *25*, 1610−1616. (d) Rithner, C. D.; Bushweller, C. H. *J. Phys. Chem.* **1986**, *90*, 5023−5028. (e) DiMeglio, C. M.; Luck, L. A.; Rithner, C. D.; Rheingold, A. L.; Elcesser, W. L.; Hubbard, J. L.; Bushweller, C. H. *J. Phys. Chem.* **1990**, *94*, 6255−6263. (f) DiMeglio, C. M.; Ahmed, K. J.; Luck, L. A.; Weltin, E. E.; Rheingold, A. L.; Bushweller, C. H. *J. Phys. Chem.* **1992**, *96*, 8765−8777.

10.1021/ic051198x CCC: $30.25
Published on Web 10/20/2005

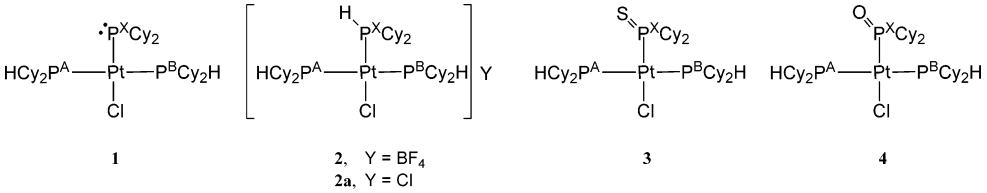

1 **2**, Y = BF_4; **2a**, Y = Cl **3** **4**

Figure 1.

$(COC_3F_7)(PPhAr)$ (^{19}F),[5] $[Pt(\eta^3\text{-}C_3H_5)(PCy_3)_2]^+$,[6] $Pt(C_2H_4)_2(PR_3)$,[7] or $[M(\eta^6\text{-arene})(CO)_2(PPh_3)]$ (M = Cr, Mo) (^{13}C).[8]

In this paper, we report on the dynamic behavior of four dicyclohexylphosphanyl Pt(II) complexes which have the *trans*-$Pt(PHCy_2)_2Cl$ moiety in common. The complexes studied are *trans*-$[Pt(Cl)(PHCy_2)_2(PCy_2)]$ (**1**), $[Pt(Cl)(PHCy_2)_3]BF_4$ (**2**), $[Pt(Cl)(PHCy_2)_3]Cl$ (**2a**), *trans*-$[Pt(Cl)(PHCy_2)_2\{\kappa P\text{-}P(S)Cy_2\}]$ (**3**), and *trans*-$[Pt(Cl)(PHCy_2)_2\{\kappa P\text{-}P(O)Cy_2\}]$ (**4**) (Figure 1). Multinuclear dynamic NMR spectroscopy gave approximate free energies of activation for the dynamic processes.[9]

Experimental Section

All manipulations of complex **1** (prepared as described in ref 10) were carried out under a pure argon atmosphere, using freshly distilled and oxygen-free solvents. Dicyclohexylphosphane (Strem) and $PtCl_2$ (Acros) were used as received. C, H, and S elemental analyses were carried out on a Eurovector CHNS−O Elemental Analyzer. Cl elemental analysis was performed by potentiometric titration using a Metrohm DMS Titrino. Melting points were measured with a Gallenkamp apparatus and were not corrected. Infrared spectra were recorded on a Bruker Vector 22 spectrometer. Thf solutions of the complexes were infused with a Cole−Parmer syringe pump. All ESI/MS spectra were recorded with an Agilent LC/MS SL series instrument adopting the following general conditions: electrospray, positive ions, flow rate 0.200 mL min^{-1}, drying gas flow 4.0 L min^{-1}, nebulizer pressure 25 psi, drying gas temperature 300 °C, capillary voltage 4000 V, mass range 400÷1400 *m*/*z*. The isotopic pattern was calculated by the Isotope Pattern Viewer software available free of charge from the www.surfacespectra.com website. NMR spectra were recorded on BRUKER Avance DRX400 spectrometer; frequencies are referenced to Me_4Si (^1H and ^{13}C), 85% H_3PO_4 (^{31}P), 1 M aqueous NaCl (^{25}Cl), and H_2PtCl_6 (^{195}Pt). The reported temperatures were calibrated from the chemical shift difference of the signals in the ^1H spectrum of a standard sample of methanol. The uncertainty in the $\Delta G^{\ddagger}_{Tc}$ values (±0.2 kcal/mol) was estimated on the basis of the assumption that there is an error of 5 °C in the determination of the coalescence temperature.

$[Pt(Cl)(PCy_2H)_3]Cl$[11] (2a). A solution of dicyclohexylphosphane (0.250 g, 1.263 mmol) in 10 mL of toluene was added to $PtCl_2$ (0.112 g, 0.421 mmol) and the resulting suspension was stirred overnight at room temperature. After the evaporation of the solvent and the addition of CH_3OH (15 mL), the resulting colorless solution was filtered through a Celite pad; then it was concentrated, and toluene was added, causing the precipitation of **2a** as a white solid. The solid was isolated by filtration and washed with *n*-hexane. Yield: 0.263 g (73%).

Alternatively, a toluene solution of dicyclohexylphosphane (0.17 g, 0.86 mmol in 5 mL) was added dropwise at room temperature to a stirred toluene suspension of *cis*-$[PtCl_2(PHCy)_2]$ (0.569 g, 0,86 mmol in 10 mL). After 6 h, the white solid formed was isolated by filtration and washed with *n*-hexane (0.614 g, 71%).

The complex is air stable, soluble in halogenated solvents, acetonitrile, alcohols, and thf, and insoluble in toluene.

Anal. Calcd for $C_{36}H_{69}Cl_2P_3Pt$: C, 50.23; H, 8.08; Cl, 8.24; P, 10.79. Found: C, 50.28; H, 8.11; Cl, 8.18; P, 10.62. ESI−MS: *m*/*z* 824.4 $[M]^+$. mp: 300 °C (dec). IR (Nujol mull, cm^{-1}): ν 2308 (w) ν(P−H), 2280 (s), 1344 (m), 1328 (w), 1296 (m), 1267 (s), 1201 (m), 1172 (s), 1126 (s), 1074 (m), 1044 (s), 1009 (vs), 918 (vs), 876 (s), 846 (s), 819 (m), 740 (m), 729 (s), 514 (s), 469 (s), 449 (m), 411 (w), 400 (m), 388 (m), 367 (m), 310 (s) ν(Pt−Cl). ^1H NMR (CD_2Cl_2, 400 MHz): δ 4.96 (m, $^1J_{P-H}$ = 395 Hz, P^X−H), 4.48 (m, $^1J_{P-H}$ = 363 Hz, $^2J_{Pt-H}$ = 87 Hz, $P^{A/B}$−H). ^{31}P NMR (CD_2Cl_2, 162 MHz): δ 5.8 (t, $^1J_{P-Pt}$ = 3137 Hz, $^1J_{P-H}$ = 395 Hz, $^2J_{PP}$ = 15 Hz, P^X), 14.8 (s, br, $^1J_{P-Pt}$ = 2215 Hz, $^2J_{P^AP^B}$ = 349 Hz, $^1J_{P-H}$ = 363 Hz, $^3J_{P-H}$ = 1.6 Hz, $P^{A/B}$). ^{195}Pt NMR (CD_2Cl_2, 86 MHz): δ −4793 (dt, $^1J_{P^X-Pt}$ = 3137 Hz, $^1J_{P^{A/B}-Pt}$ = 2215 Hz).

$[Pt(Cl)(PCy_2H)_3]BF_4$[12] (2). $AgBF_4$ (61.2 mg, 0.314 mmol) was added at room temperature to a stirred CH_2Cl_2 solution of **2a** (270 mg, 0.314 mmol, in 4 mL), causing the immediate precipitation of AgCl. After 10 min, the suspension was filtrated through a Celite

(2) Bright, A.; Mann, B. E.; Masters, C.; Shaw, B. L.; Slade, R. M.; Stainbank, R. E. *J. Chem. Soc. A* **1971**, 1826−1831. (b) Mann, B. E.; Masters, C.; Shaw, B. L.; Stainbank, R. E. *J. Chem. Soc., Chem. Commun.* **1971**, 1103−1104. (c) Attig, T. G.; Clark, H. C. *J. Organomet. Chem.* **1975**, *94*, C49−C52. (d) Faller, J. W.; Johnson, B. V. *J. Organomet. Chem.* **1975**, *96*, 99−113. (e) Empsall, H. D.; Mentzer, E.; Pawson, D.; Shaw, B. L. *J. Chem. Soc., Chem. Commun.* **1977**, 311−313. (f) Empsall, H. D.; Hyde, E. M.; Mentzer, E.; Shaw, B. L. *J. Chem. Soc., Dalton Trans.* **1977**, 2285−2291. (g) Hunter, G.; Weakley, T. J. R.; Weissensteiner, W. *J. Chem. Soc., Dalton Trans.* **1987**, 1545−1550. (h) Deeming, A. J.; Doherty, S.; Marshall, J. E. *Polyhedron* **1991**, *10*, 1857−1864. (i) Daniel, T.; Werner, H. *J. Chem. Soc., Dalton Trans.* **1994**, 221−227. (j) Deeming, A. J.; Doherty, S. *Polyhedron* **1996**, *15*, 1175−1190. (k) Deeming, A. J.; Cockerton, B. R.; Doherty, S. *Polyhedron* **1997**, *16*, 1945−1956. (l) Böttcher, H. C.; Graf, M.; Merzweiler, K. *Polyhedron* **1997**, *16*, 341−343. (m) Pelczar, E. M.; Nytko, E. A.; Zhuravel, M. A.; Smith, J. M.; Glueck, D. S.; Sommer, R.; Incarvito, C. D.; Rheingold, A. L. *Polyhedron* **2002**, *21*, 2409−2419. (n) Giannandrea, R.; Mastrorilli, P.; Palma, M.; Fanizzi, F. P.; Englert, U.; Nobile, C. F. *Eur. J. Inorg. Chem.* **2000**, 2573−2576.

(3) Fanizzi, F. P.; Lanfranchi, M.; Natile, G.; Tiripicchio, A. *Inorg. Chem.* **1994**, *33*, 3331−3339.

(4) Deeming, A. J.; Doherty, S.; Marshall, J. E.; Powell, N. I. *J. Chem. Soc., Chem. Commun.* **1989**, 1351−1353.

(5) Wicht, D. K.; Glueck, D. S.; Liable-Sands, L. M.; Rheingold, A. *Organometallics* **1999**, *18*, 5130−5140.

(6) Mann, B. E.; Musco, A. *J. Organomet. Chem.* **1979**, *181*, 439−443.

(7) Harrison, N. C.; Murray, M.; Spencer, J. L.; Stone, F. G. A. *J. Chem. Soc., Dalton Trans.* **1978**, 1337−1342.

(8) Chudek, J. A.; Hunter, G.; MacKay, R. L.; Kremminger, P.; Schlögl, K.; Weissensteiner, W. *J. Chem. Soc., Dalton Trans.* **1990**, 2001−2005.

(9) Friebolin, H. *Basic One- and Two-Dimensional NMR Spectroscopy*, 2nd ed.; VCH: New York, 1993; p 287−314.

(10) Mastrorilli, P.; Nobile, C. F.; Fanizzi, F. P.; Latronico, M.; Hu, C.; Englert, U. *Eur. J. Inorg. Chem.* **2002**, 1210−1218.

(11) Anand, S. P.; Goldwhite, H.; Spielman, J. R. *Transition Met. Chem.* **1977**, *2*, 158−160. (b) Moers, F. G.; Thewissen, D. H. M. W.; Steggerda, J. J. *J. Inorg. Nucl. Chem.* **1977**, *39*, 1321−1322.

(12) Forder, R. J.; Mitchell, I. S.; Reid, G.; Simpson, R. H. *Polyhedron* **1994**, *15*, 2129−2133.

Table 1. Crystallographic Data and Structural Refinement Details for **4**

empirical formula	$C_{36}H_{70}ClO_2P_3Pt$
formula mass	858.37
temp (K)	110(2)
wavelength (Å)	0.71073
cryst syst	triclinic
space group	$P\bar{1}$
unit cell dimensions	
a (Å)	11.9262(8)
b (Å)	13.3376(10)
c (Å)	13.4580(9)
α (deg)	101.035(2)
β (deg)	111.432(2)
γ (deg)	94.637(2)
V (Å^3)	1929.0(2)
Z	2
D_{calcd} (Mg m^{-3})	1.478
abs coeff (mm^{-1})	3.860
θ range (deg)	2.23−29.16
independent reflns	10259
observed reflns	8980
data/parameters	10259/388
GOF on F^2	1.067
R1[a] ($I > 2\sigma(I)$)	0.0402
wR2[b] (all data)	0.0890
largest diff. peak/hole [e· Å^{-3}]	2.753, −2.692 (<0.9 Å from Pt)

[a] $R1 = \sum||F_o| - |F_c||/\sum|F_o|$. [b] $wR2 = [\sum w(F_o^2 - F_c^2)^2/\sum w(F_o^2)^2]^{1/2}$.

pad, and the filtrate was evaporated in vacuo yielding pure **2** as a white solid (265 mg, 92%).

The complex is air stable, soluble in halogenated solvents, acetonitrile, alcohols, and thf, and insoluble in toluene.

Anal. Calcd for $C_{36}H_{69}BClF_4P_3Pt$: C, 47.40; H, 7.62; Cl, 3.89; P, 10.19. Found: C, 47.38; H, 7.65; Cl, 3.81; P, 10.12. mp: 265−266 °C. IR (Nujol mull, cm^{-1}): *ν* 2360 (w) *ν*(P−H), 1297 (w), 1269 (w), 1203 (w), 1180 (m), 1062 (s) *ν*(B−F from BF_4), 919 (m), 842 (m), 819 (w), 727 (w), 518 (m), 465 (w), 311 (m) *ν*(Pt−Cl). ^{1}H NMR (CD_2Cl_2, 400 MHz): *δ* 4.15 (m, $^1J_{P-H}$ = 351 Hz, $^2J_{Pt-H}$ = 86 Hz, $P^{A/B}$−H), 4.28 (m, $^1J_{P-H}$ = 385 Hz, $^2J_{Pt-H}$ = 46 Hz, P^X−H). ^{31}P NMR (CD_2Cl_2, 162 MHz): *δ* 9.9 (t, $^1J_{P-Pt}$ = 3159, $^1J_{P-H}$ = 385 Hz, $^2J_{P^{A/B}P^X}$ = 15 Hz, P^X), 16.8 (s, br, $^1J_{P-Pt}$ = 2224 Hz, $^2J_{P^AP^B}$ = 339 Hz, $^1J_{P-H}$ = 351 Hz, $^3J_{P-H}$ = 1.0 Hz, $P^{A/B}$). ^{195}Pt NMR (CD_2Cl_2, 86 MHz): *δ* −4802 (dt, $^1J_{P^X-Pt}$ = 3159 Hz, $^1J_{P^{A/B}-Pt}$ = 2224 Hz).

***trans*-[Pt(Cl)(PHCy₂)₂{κ*P*-P(S)Cy₂}] (3).** The addition of elemental sulfur (7.9 mg, 0.247 mequiv) to a stirred toluene solution of **1** (0.204 g, 0.247 mmol in 6 mL) caused the precipitation of **3** as white solid, which was isolated by filtration, washed with toluene (2 × 2 mL) and dried under vacuum. Yield: 0.176 g (83%).

The complex is air stable, poorly soluble in thf, and scarcely soluble in toluene.

Anal. Calcd for $C_{36}H_{68}ClP_3PtS$: C, 50.49; H, 8.00; Cl, 4.14; P 10.85. Found: C, 50.55; H, 7.87; Cl, 4.04; P, 10.94. mp: 204 °C (dec). ESI−MS: *m*/*z* 856.3 $[M + H]^+$. IR (Nujol mull, cm^{-1}): *ν* 2334 (w) *ν*(P−H), 1296 (w), 1264 (w), 1173 (m), 1117 (w), 1076 (w), 1005 (m), 916 (w), 888 (w), 855 (m), 814 (w), 738 (m), 579 (s) *ν*(P═S), 510 (m), 467 (w), 284 (m) *ν*(Pt−Cl). ^{1}H NMR (C_6D_6, 400 MHz): *δ* 4.63 (m, $^1J_{P-H}$ = 370 Hz, $^2J_{Pt-H}$ = 80 Hz, P−H). ^{31}P NMR (thf-d_8, 162 MHz, 325 K): *δ* 42.6 (s, $^1J_{P-Pt}$ = 3043 Hz, P^X), 34.3 (s, br, $^1J_{P-Pt}$ = 2816 Hz, $^2J_{PAPB}$ = 354 Hz, $^1J_{P-H}$ = 369 Hz, $P^{A/B}$). ^{195}Pt NMR (C_6D_6, 86 MHz): *δ* −4660 (dt, $^1J_{P^X-Pt}$ = 3010 Hz, $^1J_{P^{A/B}-Pt}$ = 2842 Hz).

***trans*-[Pt(Cl)(PHCy₂)₂{κ*P*-P(O)Cy₂}] (4).** Carefully deaerated H_2O_2 (200 *μ*L, 40% v/v) was added to a toluene solution of **1** (0.136 g, 0.165 mmol in 4 mL), and the resulting mixture was vigorously stirred for 5 min. The resulting white suspension was filtered, and the solid obtained was washed with toluene and dried under vacuum. Yield: 0.128 g (92%).

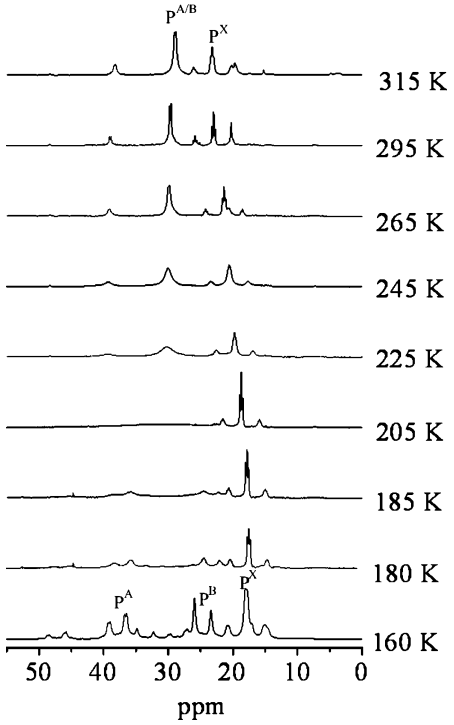

Figure 2. ^{31}P{^{1}H} DNMR of **1** (thf-d_8).

The complex is air stable, hygroscopic, soluble in halogenated solvents, alcohols, and thf, and scarcely soluble in toluene and *n*-hexane.

Anal. Calcd for $C_{36}H_{68}ClOP_3Pt$: C, 51.45; H, 8.16; Cl, 4.22; P, 11.06. Found: C, 51.37; H, 8.20; Cl, 4.19; P, 11.00. mp: 206−208 °C. ESI−MS: *m*/*z* 840.5 $[M + H]^+$. IR (Nujol, cm^{-1}): *ν* 2314 (w) *ν*(P−H), 1294 (m), 1175 (m) and 1075 (s) *ν*(P═O), 1003 (m), 916 (m), 880 (m), 850 (m), 814 (m), 543 (s), 513 (m), 390 (m), 275 (m) *ν*(Pt−Cl). ^{1}H NMR (CD_2Cl_2, 400 MHz): *δ* 4.12 (m, $^1J_{P-H}$ = 372 Hz, $^2J_{Pt-H}$ = 96 Hz). ^{31}P NMR (CD_2Cl_2, 162 MHz): *δ* 25.1 (s, br, $^1J_{P-Pt}$ = 2842 Hz, $^1J_{P-H}$ = 372 Hz, $^2J_{P^AP^B}$ = 357 Hz, $P^{A/B}$), 54.1 (t, $^1J_{P^X-Pt}$ = 3111 Hz, $^2J_{P^XP^A}$ = 16 Hz, P^X). ^{195}Pt NMR (CD_2Cl_2, 86 MHz): *δ* −4619 (dt, $^1J_{P^X-Pt}$ = 3111 Hz, $^1J_{P^{A/B}-Pt}$ = 2842 Hz).

X-ray Crystallography.[13]Crystal data, parameters for intensity data collection, and convergence results for **4** are compiled in Table 1. Data were collected with Mo Kα radiation (graphite monochromator, *λ* = 0.71073 Å) on a Bruker D8 goniometer with SMART CCD area detector at 110(2) K on a crystal with approximate dimensions of 0.17 × 0.14 × 0.05 mm. An empirical absorption correction[14] (minimum trans. 0.56, maximum trans. 0.83) was applied before averaging symmetry equivalent data (R(int) = 0.0577). The structure was solved by direct methods[15] and refined with full-matrix least-squares on F^2.[16]

(13) Crystallographic data (excluding structure factors) for the structure reported in this paper have been deposited with the Cambridge Crystallographic Data Centre as supplementary publication No. CCDC 277690. Copies of the data can be obtained free of charge by application to CCDC, 12 Union Road, Cambridge CB2 1EZ, UK. Fax: int. code + 44(1223)336−033. E-mail: deposit@ccdc.cam.ac.uk.

(14) Sheldrick, G. M. *SADABS, Program for Empirical Absorption Correction of Area Detector Data*: University of Göttingen: Göttingen, Germany, 1996.

(15) Sheldrick, G. M. *SHELXS97, Program for Crystal Structure Solution*; University of Göttingen: Göttingen, Germany, 1997.

Table 2. ^{31}P Spectroscopic Features of *trans*-[Pt(Cl)(PHCy$_2$)$_2${P(X)Cy$_2$}] Species at Low Temperature

complex	X	δ_A	δ_B	δ_X	J(A−B)	T_c (K)	$\Delta\nu$ (Hz)[a]	k_c (s^{-1})	$\Delta G^{\ddagger}$ (kcal mol^{-1})	solvent	T (K)
1	−	39.17	24.66	18.05	413	202	2350	5680	8.2	Thf-d_8	160
2	H	22.58	10.71	8.12	342	235	1923	4660	9.7	CD_2Cl_2	175
2a	H	21.00	11.40	6.10	343	240	1584	3980	10.0	CD_2Cl_2	183
2a	H	22.61	11.10	8.40	342	230	1864	4540	9.5	CD_2Cl_2/CH_3OH	165
3	S	45.99	18.12	40.84	360	225	4519	10200	8.9	Thf-d_8	160
4	O	25.49	22.00	64.49	345	248	566	2260	10.6	CD_2Cl_2/CH_3OH	170

[a] At $k_c = 0$.

Table 3. ^{1}H Spectroscopic Features of *trans*-[Pt(Cl)(PHCy$_2$)$_2${P(X)Cy$_2$}] Species at Low Temperature

complex	X	δ_A	δ_B	T_c (K)	$\Delta\nu$ (Hz)	k_c (s^{-1})	$\Delta G^{\ddagger}$ (kcal mol^{-1})	solvent	T (K)
1	−	3.95	3.89	165	24	53	8.2	Thf-d_8	160
2	H	4.03	3.85	203	75	167	9.7	CD_2Cl_2	165
3	S	5.01	4.17	200	334	743	8.9	Thf-d_8	160
4	O	4.28	3.70	235	231	513	11.0	CD_2Cl_2	170
4	O	4.06	3.74	225	127	283	10.5	CD_2Cl_2/CD_3OD	170

Results and Discussion

Dynamic Behavior of 1. Dynamic $^{31}P\{^1H\}$ NMR spectrum of *trans*-[Pt(Cl)(PHCy$_2$)$_2$(PCy$_2$)] (**1**) in thf-d_8 is reported in Figure 2. The $^{31}P\{^1H\}$ NMR signal at 295 K of the coordinated *trans*-phosphanes consists of a doublet with $\Delta\nu_{1/2} = 25$ Hz, which broadens when the temperature is lowered until 202 K, the coalescence temperature. Further lowering of the temperature causes decoalescence, with the appearance of an ABX spin system (X = terminal phosphide P) the details of which are summarized in Table 2. The coalescence temperature ($T_c = 202$ K) together with the $\Delta\nu$ between the resonances of P^A and P^B allowed us to calculate the exchange constant, k_c (5680 s^{-1}), and the activation free energy, $\Delta G^{\ddagger}$, for the dynamic process (8.2 kcal/mol).

In the dynamic ^1H spectrum, the coalescence temperature was found to be around 165 K, and at 160 K (the lowest T obtainable in thf-d_8),[17] the P−H signal separated into two broad doublets ($\delta_{P^A-H} = 3.95$, $^1J_{P-H} = 380$ Hz; $\delta_{P^B-H} = 3.89$, $^1J_{P-H} = 360$ Hz). These features indicate an approximate $\Delta G^{\ddagger}$ value identical to that calculated from $^{31}P\{^1H\}$ DNMR analysis (Table 3).

The dynamic behavior observed for **1** can be, in principle, the result of two determinants: (i) a slow phosphorus inversion in the pyramidal phosphide ligand and (ii) the presence of several slowly interconverting rotamers because of hindered rotation around the Pt−P^X bond.

These two hypotheses cannot be easily distinguished since, in our system, their effect on the NMR features is the same.

In fact, the observed appearance of an ABX spin system indicates only that, on lowering the temperature, *both* the P^X inversion *and* the rotation about the P^X−Pt bond become slow. However, the value of $\Delta G^{\ddagger}$ of 8.2 kcal/mol found for **1** is sensibly lower than those usually found for inversions in related terminal phosphide complexes. Typical values for $\Delta G^{\ddagger}$ for dynamic processes involving terminal phosphides bound to metals such as Re,[18] Fe,[19] Nb,[20] Ir,[21] W,[22] Pd,[23] and Pt,[5,23,24] range between 10.9 and 18.0 kcal/mol.

In the case of complex **1**, both steric and electronic factors should further increase the inversion barrier. In fact, although bulky cyclohexyl substituents should lower the P inversion barrier,[25] the latter is increased because the clear P^X pyramidal geometry found in the X-ray crystal structure of **1** (sum of the angles at P of 320.5°,[10] compared to 328.5° for a tetrahedral atom and 360° for a planar atom) increases the energy difference between the planar transition state for the inversion and the pyramidal ground state.

As for the electronic effects that affect the inversion barrier, our crystallographic and ^{31}P NMR results[10] point out a low s character of the P^X−Pt bond in **1** which should lead to a high inversion barrier because of the rehybridization energy necessary to reach the sp^2 transition state.[26] Taking the $^{31}P^X$—^{195}Pt coupling constant as a probe of the s character of the P^X−Pt bond (the lower the constant, the lower the s character)[5] and the 1102−1112 Hz $^1J_{^{31}P^X-^{195}Pt}$ value found for cyclometalated dimesityl phosphide Pt(II) complexes (for which pure inversion barriers of ca. 13 kcal/mol have been calculated),[23] an inversion barrier higher than 13 kcal/mol

(16) Sheldrick, G. M. *SHELXL97, Program for Crystal Structure Refinement*; University of Göttingen: Göttingen, Germany, 1997.
(17) Complex **1**, as well as **3**, reacts in halogenated solvents that therefore could not be used in the low-temperature NMR experiments.
(18) Simpson, R. D.; Bergman, R. G. *Organometallics* **1992**, *11*, 1980−1993. (b) Zwick, B. D.; Dewey, M. A.; Knight, D. A.; Buhro, W. E.; Arif, A. M.; Gladysz, J. A. *Organometallics* **1992**, *11*, 2673−2685. (c) Buhro, W. E.; Zwick, B. D.; Georgiou, S.; Hutchinson, J. P.; Gladysz, J. A. *J. Am. Chem. Soc.* **1988**, *110*, 2427−2439. (d) Buhro, W. E.; Gladysz, J. A. *Inorg. Chem.* **1985**, *24*, 3505−3507.
(19) Malisch, W.; Gunzelmann, N.; Thirase, K.; Neumayer, M. *J. Organomet. Chem.* **1998**, *571*, 215−222. (b) Crisp, G. T.; Salem, G.; Wild, S. B.; Stephens, F. S. *Organometallics* **1989**, *8*, 2360−2367.
(20) Bonnet, G.; Kubicki, M. M.; Moise, C.; Lazzaroni, R.; Salvadori, P.; Vitulli, G. *Organometallics* **1992**, *11*, 964−967.
(21) Fryzuk, M. D.; Joshi, K.; Chadha, K.; Rettig, S. J. *J. Am. Chem. Soc.* **1991**, *113*, 8724−8736.
(22) Malisch, W.; Maisch, R.; Meyer, A.; Greissinger, D.; Gross, E.; Colquhoun, I. J.; McFarlane, W. *Phosphorus, Sulfur Silicon Relat. Elem.* **1983**, *18*, 2299−2302.
(23) Zhuravel, M. A.; Glueck, D. S.; Zakharov, L. N.; Rheingold, A. L. *Organometallics* **2002**, *21*, 3208−3214.
(24) Wicht, D. K.; Kovacik, I.; Glueck, D. S.; Liable-Sands, L. M.; Incarvito, C. D.; Rheingold, A. L. *Organometallics* **1999**, *18*, 5141−5151.
(25) Rauk, A.; Allen, L. C.; Mislow, K. *Angew. Chem., Int. Ed. Engl.* **1970**, *9*, 400−414.
(26) Wicht, D. K.; Paisner, S. N.; Lew, B. N.; Glueck, D. S.; Yap, G. P. A.; Liable-Sands, L. M.; Rheingold, A.; Haar, C. M.; Nolan, S. P. *Organometallics* **1998**, *17*, 652−660.

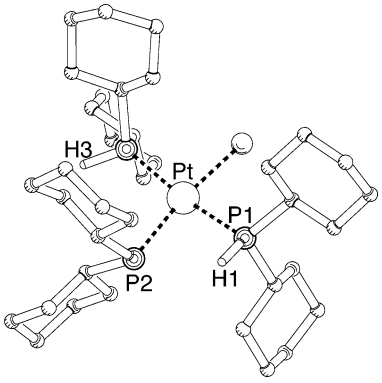

Figure 3. PLUTON[28] view of the rotamer found in the crystal of **1**.

has to be expected for **1**, the $^1J_{^{31}P^X-^{195}Pt}$ value of which is 929 Hz (thf-d_8, 295 K).

Moreover, theoretical calculations show that, contrary to the case of early transition metal phosphides, in Fe(II)−PR$_2$ complexes, the rotational barrier is always much lower than the inversion barrier.[27]

In light of these considerations, we favor the rotational process as the predominant process in determining the activation barrier for **1**, that is $\Delta G^{\ddagger}_{inv} \gg \Delta G^{\ddagger}_{rot}$ so that, at room temperature, rotation is fast and inversion is slow. Lowering the temperature would gradually lock the inversion and slow the rotation. If this interpretation is correct, the coalescence temperature would refer to a situation in which the inversion is already locked and the rotation rate is on the order of the NMR time scale.

We believe that the rotamer stable at low temperatures is the sterically least hindered conformer depicted in Figure 3 and found in the crystal.[10]

Dynamic Behavior of 2, 3, and 4. To confirm our assignment of $\Delta G^{\ddagger}$ predominantly to the rotational process, we decided to compare the dynamic behavior of **1** with that of complexes [Pt(PHCy$_2$)$_3$Cl]BF$_4$ (**2**), *trans*-[Pt(Cl)(PHCy$_2$)$_2$-{κP-P(S)Cy$_2$}] (**3**), and *trans*-[Pt(Cl)(PHCy$_2$)$_2${κP-P(O)Cy$_2$}] (**4**), which have the same *trans*-Pt(PHCy$_2$)$_2$Cl moiety and differ from **1** in the substituent on P^X (Figure 1).

All three complexes are characterized by a broad $^{31}P\{^1H\}$ NMR signal for the P$^{A/B}$HCy$_2$ at 295 K [$\Delta\nu_{1/2}$ = 100 Hz (CD_2Cl_2), 190 Hz (thf-d_8), and 76 Hz (CD_2Cl_2), for **2**, **3**, and **4,** respectively]. For complexes **2**−**4**, the dissociation equilibrium of a coordinated PHCy$_2$ was also considered as a possible factor responsible for the observed broadness of the P$^{A/B}$ signals. However, since no trace of free PHCy$_2$ was observed by $^{31}P\{^1H\}$ NMR in the range of temperatures (160−325 K) used for this study, the only dynamic process held responsible for signal broadening was restricted rotation about the Pt−P^X bond.[29]

Cationic complex **2** was obtained as the tetrafluoroborate salt by reaction of *cis*-[PtCl$_2$(PHCy$_2$)$_2$] with PCy$_2$H and AgBF$_4$, and it had a behavior similar to that found for **1** for the dynamic $^{31}P\{^1H\}$ NMR. The coalescence temperature was 235 K and the calculated $\Delta G^{\ddagger}$ for the rotation around P^X−Pt bond was 9.7 kcal/mol (Tables 2−3).

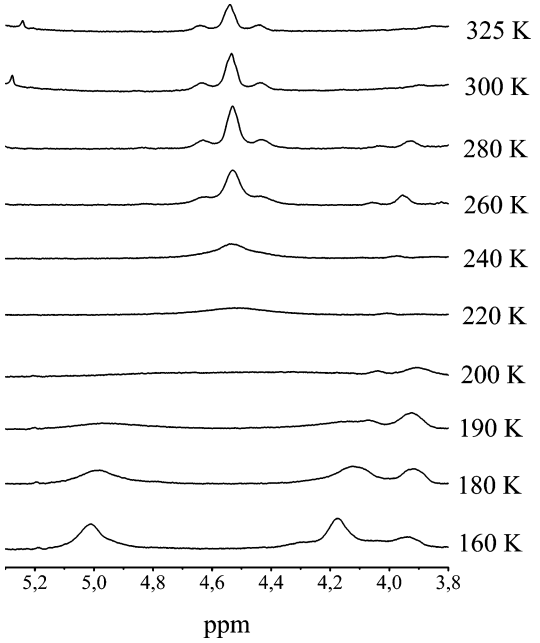

Figure 4. $^1H\{^{31}P\}$ DNMR spectrum of **3** (thf-d_8).

Phosphanylsulfide complex **3** was obtained by reaction of **1** with 1 equiv of sulfur in toluene. Variable-temperature $^{31}P\{^1H\}$ NMR spectra were recorded in the temperature range of 160−325 K. The proton-coupled ^{31}P NMR spectrum at 325 K gave sufficiently sharp lines for the $[AXY_2]_2M^{30}$ spin system (A is P$^{A/B}$, X is the proton bound to P$^{A/B}$, Y represents the methyne protons of the cyclohexyl rings bound to P$^{A/B}$, and *M* is P^X) to be analyzed for spectroscopic features (see Experimental Section). Low-temperature $^{31}P\{^1H\}$ NMR spectra showed the expected broadening of the PCy$_2$H signal which gave coalescence at 225 K and separated in the AB system (with ^{195}Pt satellites) at 160 K. The values calculated for the k_c and $\Delta G^{\ddagger}$ are 10200 s^{-1} and 8.9 kcal/mol, respectively (Tables 2−3). A 200 K coalescence temperature was found by dynamic $^1H\{^{31}P\}$ NMR analysis (Figure 4) which again gave a $\Delta G^{\ddagger}$ value of 8.9 kcal/mol.

Phosphanyloxide complex **4**, a side product of the aerobic oxidation of **1**,[31] was selectively obtained by reaction of **1** with hydrogen peroxide. Variable-temperature $^{31}P\{^1H\}$ NMR spectra and its dynamic $^{31}P\{^1H\}$ NMR behavior in CD_2Cl_2 are reported in Figure 5. When the temperature is lowered to 235 K, the expected broadening and separation of PCy$_2$H signals is observed.

However, the separation of the PCy$_2$H signals was markedly less pronounced than in previous cases (less than 1.5 ppm in **4** vs 27 ppm in **3**).

Interestingly, a further decrease of the temperature to 160 K in the case of compound **4**, resulted in an unexpected reapproaching of the P$^{A/B}$ signals, concomitant with their

(27) Rogers, J. R.; Wagner, T. P. S.; Marynick, D. S. *Inorg. Chem.* **1994**, *33*, 3104−3110.
(28) Spek, A. L. *PLATON-98*; University of Utrecht: Utrecht,The Netherlands, 1998.
(29) Little PHCy$_2$ dissociation was observed at room temperature when **2** was dissolved in 1,2-dichloroethane or when **3** was dissolved in halogenated solvents.
(30) Palmer, R. A.; Whitcomb, D. R. *J. Magn. Res.* **1980**, *39*, 371−379.
(31) Mastrorilli, P.; Latronico, M.; Nobile, C. F.; Suranna, G. P.; Fanizzi, F. P.; Englert, U.; Ciccarella, G. *Dalton Trans.* **2004**, 1117−1119.

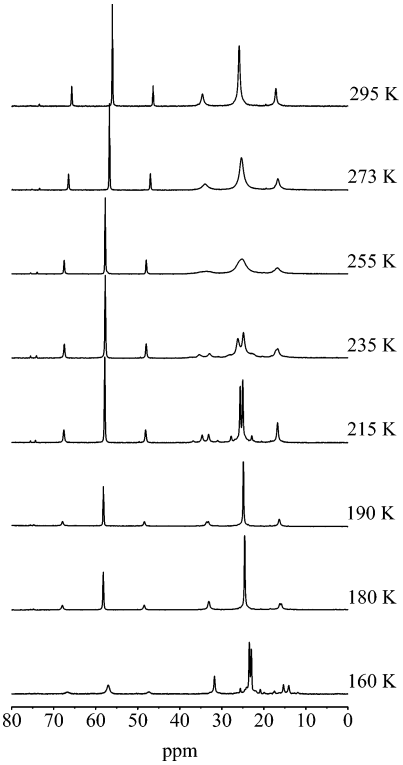

Figure 5. $^{31}P\{^1H\}$ DNMR of **4** (CD_2Cl_2).

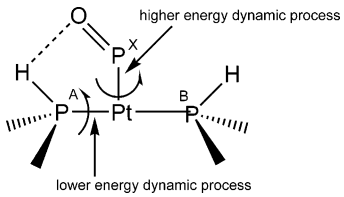

Figure 6. Alleged molecular motions of **4**.

sharpening. This behavior prevented the calculation of the $\Delta G^{\ddagger}$ from the ^{31}P NMR data. On the other hand, the dynamic $^1H\{^{31}P\}$ NMR analysis for **4** showed coalescence of the P*H* signal at 235 K and splitting of the P*H* signal (δ 4.12 at 295 K) into two peaks centered at δ 4.3 and 3.7 (T < 225 K). From these data, a 11.0 kcal/mol $\Delta G^{\ddagger}_{rot}$ could be calculated (Table 3). This relatively high $\Delta G^{\ddagger}_{rot}$ value suggested the presence of P−*H*···*O*═P intramolecular interactions in the case of compound **4** (Figure 6).

The reapproaching of the ^{31}P signals observed upon lowering the temperature from 235 to 180 K may be caused by the occurrence of two dynamic processes with different activation energies. Of these, the one at higher energy is presumably the hindered rotation about the P^X−Pt bond, analogous to that observed for compounds **1**−**3**, while the one at lower energy could be the rotation about the P^A−Pt bond (Figure 6). The latter could be slowed only in the case of **4** because of the aforementioned P−*H*···*O*═P interaction and could be responsible for the broadening of the $^{31}P^X$ NMR signal at 160 K (Figure 5).

To confirm the existence of the P−*H*···*O*═P interaction in the solid state, a crystallographic analysis was performed. X-ray diffraction studies were carried out on a single crystal obtained by slow evaporation of a 1,2-dichloroethane solution. The molecular structure is depicted in Figure 7. The distorted square planar geometry at the platinum center in **4** is similar to that in complex **1**. The Pt−P distances of the coordinated dicyclohexylphosphanes [2.2997(11) and 2.3104(11) Å] are slightly longer than that of Pt−P(O)Cy_2 [2.2688(10) Å] as a consequence of the greater trans influence of P with respect to Cl. The two P−H bonds of the $PHCy_2$ ligands are both oriented toward the P^X (P1) ligand, one of them being directed toward the oxygen bound to P^X. In comparison to related P-bound P(O)R_2−Pt complexes [Pt(Ph){κP-P(O)Ph_2}(RCN)(PPh_3)] {R = 9-anthracenyl or 3,5-dichloro-2,4,6-trimethylphenyl, P−O distance = 1.51(1) Å},[32] *anti*-[Pt($PMePh_2$){κP-P(O)Ph_2}(μ-NH_2)]$_2$ {P−O distance = 1.526(11) Å},[33] [PtL{κP-P(O)Ph_2}Cl] {L = (+)−(1*S*,2*R*)-2-(dimethylamino)-1-phenyl-1-diphenyl-phosphinoxypropane, P−O distance = 1.501(4) Å},[34] and [(PMe_2Ph){κP-P(O)Me_2}Pt(μ-NPh)]$_2$ {P−O distance = 1.509(2) Å},[35] the P−O bond distance of **4** [1.516(3) Å] is typical for a double P−O bond.

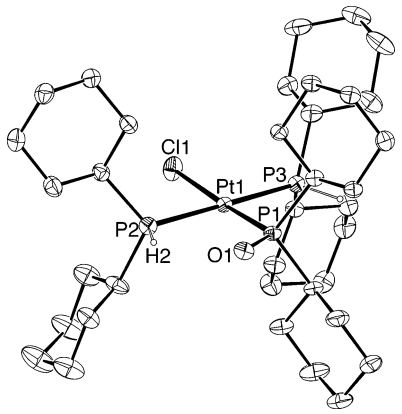

Figure 7. PLATON[28] drawing of **4**; displacement ellipsoid are scaled to 50% probability, and the hydrogen atoms bonded to C have been omitted for clarity. Selected interatomic distances (Å) and angles (deg): Pt−P(1) = 2.2688(10), Pt−P(2) = 2.2997(11), Pt−P(3) = 2.3104(11), Pt−Cl = 2.4131(10), P−O = 1.516(3), P(1)−Pt−P(2) = 91.29(4), P(1)−Pt−P(3) = 93.74(4), P(2)−Pt−P(3) = 174.45(4), P(1)−Pt−Cl = 176.23(4), P(2)−Pt−Cl = 88.51(4), P(3)−Pt−Cl = 86.61(4).

The potential H donor O1 lies only 0.12 Å above the plane defined by Pt1, P1, and P2; this close coplanarity allows for an, albeit quite weak, hydrogen bond between O1 and H2. A more complete picture of the hydrogen bonds in **4** must take the intermolecular interactions into account. The asymmetric unit in space group $P\bar{1}$ contains one molecule of water per complex. Two pairs of water and complex molecules, related by crystallographic inversion, form an overall hydrogen-bond pattern which can be described by the graph set symbol $R_4^2(8)$.[36] Figure 8 provides a graphical description of this arrangement and gives important interatomic distances.

(32) Beck, W.; Keubler, M.; Leidl, E.; Nagel, U.; Schaal, M.; Cenini, S.; Del Buttero, P.; Licandro, E.; Maiorana, S.; Chiesi-Villa, A. *J. Chem. Soc., Chem. Commun.* **1981**, 446−448.
(33) Alcock, N. W.; Bergamini, P.; Kemp, T. J.; Pringle, P. G. *J. Chem. Soc., Chem. Commun.* **1987**, 235−236.
(34) Franciò, G.; Arena, C. G.; Panzalorto, M.; Bruno, G.; Faraone, F. *Inorg. Chim. Acta* **1998**, *277*, 119−126.
(35) Li, J. J.; Li, W.; James, A. J.; Holbert, T.; Sharp, T. P.; Sharp, P. R. *Inorg. Chim.* **1999**, *38*, 1563−1572.
(36) Etter, M. C.; MacDonald, J. C.; Bernstein, J. *Acta Crystallogr.* **1990**, *B46*, 256−262. (b) Grell, J.; Bernstein, J.; Tinhofer, G. *Acta Crystallogr.* **1999**, *B55*, 1030−1043.

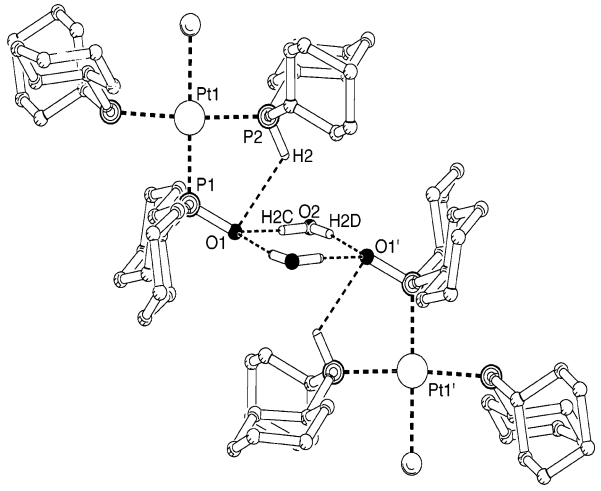

Figure 8. PLUTON[28] representation of the hydrogen-bond pattern in **4**. Selected interatomic distances (Å) and angles (deg): P(2)−H(2) = 1.12, P(2)···O(1) = 3.188(4), O(1)···H(2) = 2.492, P(2)−H(2)···O(1) = 119, O(2)−H(2C) = 0.93, O(2)···O(1) = 2.806(5), O(2)−H(2C)···O(1) = 167, O(2)−H(2D) = 0.94, O(2)···O(1′) = 2.846(5), O(2)−H(2D)···O(1′) = 173. Primed atoms are related to unprimed ones by inversion.

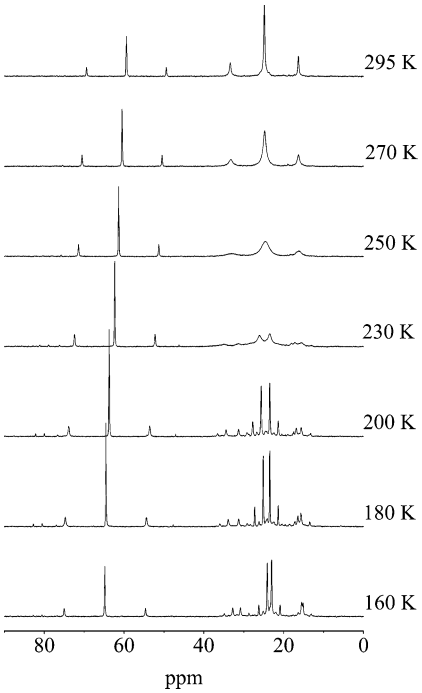

Figure 9. $^{31}P\{^{1}H\}$ DNMR of **4** (CD_2Cl_2/CH_3OH).

To gain insight into the possible intramolecular H···O interaction in solution for **4**, we have added few drops of CH_3OH to a CD_2Cl_2 solution of **4** and carried out multinuclear dynamic NMR experiments on the resulting mixture. The $^{31}P\{^{1}H\}$ spectra at variable temperatures (Figure 9) showed a much less-marked reapproaching of signals which could be related to the slowed lower-energy dynamic process (i.e., rotation about the P^A−Pt bond). This reapproaching started at 200 K but did not prevent the calculation of the higher $\Delta G^{\ddagger}_{rot}$ from ^{31}P NMR data. Moreover, in these conditions, no broadening of the $^{31}P^X$ NMR signal was observed at very low temperature.

In the CD_2Cl_2/CH_3OH mixture, the coalescence temperatures found for **4** by $^{31}P\{^{1}H\}$ and $^{1}H\{^{31}P\}$ DNMR experiments were 248 and 225 K, respectively. The corresponding $\Delta G^{\ddagger}_{rot}$ values were 10.6 (from $^{31}P\{^{1}H\}$ DNMR) and 10.5 kcal/mol (from $^{1}H\{^{31}P\}$ DNMR).

Table 4. Effect of the Solvent on the Chemical Shifts of $[Pt(Cl)(PHCy_2)_3]Cl$ (**2a**)[a]

solvent	δ_{P^X}	$\delta_{P^{A/B}}$	dielectric constant at 20 °C
CD_2Cl_2	5.4 (9.9)	14.3 (16.8)	9.1
CH_3OH	9.8 (9.9)	14.7 (15.8)	33.6
CH_3CN	9.6 (10.4)	15.1 (15.6)	36.6
CD_2Cl_2 with two drops of CD_3OD	10.1 (10.7)	17.1 (17.1)	

[a] Values in parentheses refer to $[Pt(Cl)(PHCy_2)_3]BF_4$ (**2**).

Interactions Involving the Cationic Fragment $[Pt(Cl)(PHCy_2)_3]^+$ and the Counteranion. Finally, we have considered the influence on the dynamic behavior of $[Pt(Cl)(PHCy_2)_3]^+$ of a counteranion, such as chloride, capable of interacting with the coordinated P−*H* more strongly than BF_4^-.

From the DNMR experiments, a $\Delta G^{\ddagger}_{rot}$ of 10.0 kcal/mol was calculated for the complex $[Pt(Cl)(PHCy_2)_3]Cl$ (**2a**), a value slightly higher than that obtained for **2**. This can be interpreted by admitting that in the case of **2a** there is a small contribution to $\Delta G^{\ddagger}_{rot}$ resulting from a P*H*···*Cl*$^-$ interaction,[37] but the small difference between the $\Delta G^{\ddagger}_{rot}$ values does not permit conclusive statements. However, other circumstantial NMR features reinforce this hypothesis.

Data collected in Table 4 show that, in contrast to what is observed for **2**, the $^{31}P^X$ chemical shift of **2a** depends on the solvent. A upfield shift with respect to **2** is observed in CD_2Cl_2, a solvent with a low dielectric constant (and therefore poor solvating ability for Cl^-).

The addition of few drops of methanol to a CD_2Cl_2 solution of **2a** caused ion-pair breaking and resulted in $^{31}P^X$ chemical shift (δ = 10.1) and $\Delta G^{\ddagger}_{rot}$ (9.5 kcal/mol) values very similar to those found for **2**.

An analogous effect was observed in the ^{1}H NMR spectra where the chemical shift of P^XHCy_2 passed from δ 4.96 to 4.38 upon addition of methanol, the corresponding value for **2** in CD_2Cl_2 being δ 4.28.

The interaction between the Pt(II) cation and Cl^- counteranion could also be evidenced by ^{35}Cl NMR spectroscopy.

The relaxation rate is related to the line width according to

$$\Delta\nu_{1/2} = \frac{1}{\pi T_2}$$

In the liquid state, extreme narrowing conditions apply, and the relaxation rates for ^{35}Cl (I = 3/2) are given by

$$\frac{1}{T_1} = \frac{1}{T_2} = \frac{2\pi^2}{5h^2}\left(1 + \frac{\eta^2}{3}\right)(eQq)^2\tau_c$$

where η is the asymmetry parameter, Q is the nuclear quadruple moment, τ_c is the correlation time for molecular

(37) A hydrogen bond between a P−H and the Cl^- has been reported in ref 18b for $[Re(Cp)(NO)(PPh_3)(PPhH_2)]$ both in solution and in the solid state.

reorientation, and q is the electric field gradient at the nucleus. This field results from the charge distribution around the nucleus (i.e., the surrounding electrons and nearby nuclei). Because of the spherical symmetry of the electron cloud, the field gradient at the ^{35}Cl nucleus in free $Cl^-_{(g)}$ should be zero. When the chloride ion is in solution, its solvation shell generates a fluctuating field gradient at the nucleus. This gradient will not be large because solvent molecules are disposed about the ion in an approximately symmetrical way, and in solution, the free Cl^- should give a ^{35}Cl NMR signal only a few Hz wide. The approach of a counterion destroys the symmetry of the solvation shell and increases the field gradient at the ^{35}Cl nucleus.[38] The magnitude of the field gradient caused by the counterion is strongly dependent on interionic distance. In the point charge model, the ^{35}Cl NMR line width is proportional to the sixth power of the $Cl^-\cdots$counterion distance:[39] therefore, in a contact ion pair a large field gradient will be generated at the ^{35}Cl nucleus, with a consequently great enhancement of the relaxation, also the result of the relatively high value of Q ($-0.082\cdot10^{-28}$ m^2). The result is a very broad ^{35}Cl NMR signal which could disappear in the rolling of the spectrum baseline. Given that contact-ion pairing can be detected by examining the ^{35}Cl NMR line width as a function of concentration,[40] we have recorded ^{35}Cl NMR spectra of CD_2Cl_2 solutions of **2a** in the $8.2 \times 10^{-3}-6.2 \times 10^{-2}$ range of concentration, but in any case, no ^{35}Cl signal was detected. More diluted solutions were not considered because of the low ^{35}Cl NMR sensitivity (3.55×10^{-3} vs ^{1}H). As expected, the addition of one drop of methanol caused the appearance of an intense ^{35}Cl NMR signal centered at δ -21, thus supporting the existence of a P*H*$\cdots$*Cl*$^-$ interaction being responsible for the different $\Delta G^{\ddagger}_{rot}$ values found for **2** and **2a**.

Conclusions

The comparison of the activation free energies collected in Table 2 permits the following considerations. The least value found for **1** is what one would expect for the hindered rotation around the Pt$-$P^X bond (at locked inversion) on the basis of steric reasons. In fact, the terminal phosphido complex **1** is characterized by the longest expected Pt$-$P^X bond [^1J(P$-$Pt) = 929 Hz for **1** vs 3159 (**2**), 3034 (**3**), and 3245 Hz (**4**)] and the least hindered substituent among the series X = lone pair, H, S, O. The highest value found for **4** (11.0 kcal/mol) can be the result of the presence of a P$-$*H*$\cdot\cdot$*O*=P intramolecular interaction that, below 235 K, might result in a slowing of the rotation about the P$^A-$Pt bond. The addition of a hydrogen bond breaker, such as CH_3OH, lowered the energy barrier for the rotation about the P$^X-$Pt bond (which became 10.5 kcal/mol) and increased the energy gap of the two dynamic processes (i.e., rotation about the P$^X-$Pt and P$^A-$Pt bonds). Single-crystal X-ray diffraction confirmed the presence of both *intra* and *inter*molecular P=O$\cdots$H interactions in solid **4**. For complex **2a**, the presence of ion pairing between P^{X}HCy$_2$ and the Cl^- counteranion has been proven by multinuclear NMR.

Acknowledgment. Dr. G. Ciccarella is gratefully acknowledged for the ESI$-$MS analyses. A grant from Italian MIUR (PON Project 2000$-$2006 No. 3043/45) for the purchase of the 400 MHz NMR spectrometer is acknowledged. Italian MIUR (PRIN 2004, Project 2004030719_005) is gratefully acknowledged for financial support.

Supporting Information Available: ESI$-$MS spectra of [Pt(Cl)(PHCy$_2$)$_3$]$^+$ for **3** and **4**, ^{31}P{^{1}H} NMR spectra of **2**, **2a**, and **3**, atomic coordinates, equivalent isotropic displacement parameters, and bond lengths and angles for **4**. This material is available free of charge via the Internet at http://pubs.acs.org.

IC051198X

(38) Berman, H. A.; Stengle, T. R. *J. Phys. Chem.* **1975**, *79*, 1001$-$1005.
(39) Barnes, R. G.; Smith, W. V. *Phys. Rev.* **1954**, *93*, 95$-$98. (b) Townes, C. H.; Dailey, B. P. *J. Chem. Phys.* **1952**, *20*, 35$-$40.
(40) Avent, A. G.; Chalouer, P. A.; Day, M. P.; Seddon, K. R.; Welton, T. *J. Chem. Soc., Dalton Trans.* **1994**, 3405$-$3413.